Inorganic Chemistry
Communication

Inorg. Chem. **2009**, *48*, 9051–9053 **9051**
DOI: 10.1021/ic9007526

Effect of Magnetic Dipole−Dipole Interactions on the Spin Orientation and Magnetic Ordering of the Spin-Ladder Compound $Sr_3Fe_2O_5$

Hyun-Joo Koo,*,† Hongjun Xiang,‡ Changhoon Lee,§ and Myung-Hwan Whangbo*,§

†*Department of Chemistry and Research Institute of Basic Science, Kyung Hee University, Seoul 130-701, Korea,* ‡*National Renewable Energy Laboratory, Golden, Colorado 80401, and* §*Department of Chemistry, North Carolina State University, Raleigh, North Carolina 27695*

Received April 18, 2009

First-principles density functional theory calculations show that the spin−lattice of $Sr_3Fe_2O_5$ is practically 2D in terms of its spin-exchange interactions. The magnetic dipole−dipole interactions are found to be essential for the 3D magnetic ordering of $Sr_3Fe_2O_5$ at a very low temperature.

The preferred spin orientations of the magnetic ions in a given magnetic solid are governed by several factors, namely, spin−orbit coupling (SOC), spin exchange (SE), antisymmetric (AS), and magnetic dipole−dipole (MDD) interactions (Figure 1). The SOC affects the spin orientation of a single magnetic ion,[1,2] while the SE interactions control the relative orientations of the spins such that they are collinear if there is no severe spin frustration in the SE interactions but become noncollinear (e.g., compromised and spiral spin arrangements) otherwise.[3,4] The AS interaction arises from a combined effect of the SOC and SE interactions[1,5] and induces spin canting, for example, from a collinear spin arrangement. The SOC, SE, and AS interactions are short-range interactions, whereas the MDD interaction is a long-range interaction. The MDD interaction is weak, being on the order of 0.1 meV for two spin $^1/_2$ ions separated by 2 Å,[6] but is responsible for the formation of various ferromagnetic (FM) domains in an FM material.[6]

In discussions of the 3D magnetic order and the spin orientation of a magnetic solid, the MDD interaction is often neglected. However, this interaction can become non-negligible if the spin S of a magnetic ion is large, because the MDD interaction is proportional to S^2. Thus, the spin ice behavior of the frustrated magnetic pyrochlore compounds $Dy_2Ti_2O_7$ and $Ho_2Ti_2O_7$ (with Ho^{3+} f^{10} and Dy^{3+} f^9 ions, respectively) at a very low temperature is explained in terms of the MDD interactions.[7] It is an open question as to whether there is any d-electron magnetic system whose spin orientation and magnetic ordering are governed by MDD interactions. As a likely candidate for such a system, we consider the ternary iron oxide $Sr_3Fe_2O_5$, which consists of Fe_2O_5 ladder chains made up of corner-sharing FeO_4 square planes with a high-spin Fe^{2+} d^6 ($S = 2$) ion (Figure 2a,b).[8] At 4 K, the Mössbauer spectrum of $Sr_3Fe_2O_5$ indicates a 3D antiferromagnetic (AFM) order and the neutron powder diffraction of $Sr_3Fe_2O_5$ reveals a ($2a$, $2b$, c) superstructure with an iron moment parallel to the c direction, i.e., the rung direction of the spin ladder (Figure 2c). Two important questions arise from this observation: (a) Is the MDD interaction responsible for the 3D AFM ordering of $Sr_3Fe_2O_5$? (b) Why does the spin orientation prefer the c direction rather than the b direction (Figure 2d) or the a direction. In the following, we probe these two questions.

We first examine the 3D AFM ordering of $Sr_3Fe_2O_5$ from the viewpoint of its five SE paths J_1-J_5. These parameters are evaluated on the basis of first-principles density functional theory (DFT) electronic structure calculations for the six ordered spin states of $Sr_3Fe_2O_5$ depicted in Figure 3, where the spin arrangement presented has either the AFM or FM arrangement between adjacent sheets of spin ladders along the a direction. Our spin-polarized DFT calculations employed the projected augmented-wave method encoded in the Vienna ab initio simulation package,[10] the generalized gradient approximation (GGA) for the exchange-correlation correction,[11] the plane-wave cutoff energy of 400 eV, a set of $8 \times 8 \times 2$ k points, and the threshold 10^{-6} eV for self-consistent-field (SCF) energy convergence. The strong electron correlation associated with the Fe 3d states was taken care of by performing GGA plus onsite repulsion (GGA + U) calculations[12] with $U = 4.6$ eV, the value used for the study of $SrFeO_2$.[13] The spin orientations of the magnetic ground state were examined by performing GGA + U + SOC calculations.

*To whom correspondence should be addressed. E-mail: hjkoo@khu.ac.kr (H.-J.K.), mike_whangbo@ncsu.edu (M.-H.W.).

(1) Dai, D.; Xiang, H. J.; Whangbo, M.-H. *J. Comput. Chem.* **2008**, *29*, 2187.
(2) Wang, X.; Wu, R.; Wang, D.-S.; Freeman, A. J. *Phys. Rev. B* **1996**, *54*, 61.
(3) Greedan, J. E. *J. Mater. Chem.* **2001**, *11*, 37 and references cited therein.
(4) Dai, D.; Whangbo, M.-H. *J. Chem. Phys.* **2004**, *121*, 672.
(5) Moriya, T. *Phys. Rev. Lett.* **1960**, *4*, 228.
(6) Ashcroft, N. W.; Mermin, N. D. *Solid State Physics*; Saunders CollegePhiladelphia, PA, 1976; pp 673−674.
(7) Bramwell, S. T.; Gingras, M. J. P. *Science* **2001**, *294*, 1495 and references cited therein.
(8) Kageyama, H.; Watanabe, T.; Tsujimoto, Y.; Kitada, A.; Sumida, Y.; Kanamori, K.; Yoshimura, K.; Hayashi, N.; Muranaka, S.; Takano, M.; Ceretti, M.; Paulus, W.; Ritter, C.; André, G. *Angew. Chem., Int. Ed.* **2008**, *47*, 5740.
(9) Tsujimoto, Y.; Tassel, C.; Hayashi, N.; Watanabe, T.; Kageyama, H.; Yoshimura, K.; Takano, M.; Ceretti, M.; Ritter, C.; Paulus, W. *Nature* **2007**, *450*, 06382.
(10) (a) Kresse, G.; Hafner, J. *Phys. Rev. B* **1993**, *62*, 558. (b) Kresse, G.; Furthmüller, J. *Comput. Mater. Sci.* **1996**, *6*, 15. (c) Kresse, G.; Furthmüller, J. *Phys. Rev. B* **1996**, *54*, 11169.
(11) Perdew, J. P.; Burke, S.; Ernzerhof, M. *Phys. Rev. Lett.* **1996**, *77*, 3865.
(12) Dudarev, S. L.; Botton, G. A.; Savrasov, S. Y.; Humphreys, C. J.; Sutton, A. P. *Phys. Rev. B* **1998**, *57*, 1505.
(13) Xiang, H. J.; Wei, S.-H.; Whangbo, M.-H. *Phys. Rev. Lett.* **2008**, *100*, 167207.

Published on Web 08/31/2009

$$\text{SOC:}\quad \lambda\vec{S}\cdot\vec{L}$$
$$\text{SE:}\quad -\sum_{i<j} J_{ij}\vec{S}_i\cdot\vec{S}_j$$
$$\text{AS:}\quad \vec{D}\cdot(\vec{S}_i\times\vec{S}_j)$$
$$\text{MDD:}\quad \left(\frac{g^2\mu_B^2}{a_0^3}\right)\left(\frac{a_0}{r_{ij}}\right)^3\left[-3(\vec{S}_i\cdot\vec{e}_{ij})(\vec{S}_j\cdot\vec{e}_{ij})+(\vec{S}_i\cdot\vec{S}_j)\right]$$

Figure 1. Four interactions governing the spin orientation of magnetic ions in space: In the SOC interaction, λ is the SOC constant, with $\hat{S}$ and $\hat{L}$ representing the spin and orbital angular momentum operators of a given spin site, respectively. In the SE interaction, J_{ij} is the parameter associated with the SE between the spin sites i and j, respectively. In the AS interaction, the Dzyaloshinsky−Moriya vector $\vec{D}$ arises from the difference in the unquenched orbital angular momenta on the two spin sites i and j.[1] In the MDD interaction, g is the electron g factor, μ_B is the Bohr magneton, a_0 is the Bohr radius (0.529 177 Å), r_{ij} is the distance between the spin sites i and j, and $\vec{e}_{ij}$ is the unit vector along the distance.

Table 1 summarizes the relative energies, per the ($2a$, $2b$, c) supercell [i.e., per eight formula units (FUs)], of the ordered spin states of $Sr_3Fe_2O_5$ obtained from the GGA + U calculations. The A3* state is found to be the magnetic ground state in agreement with experiment.[8] To extract the values of the SE parameters J_1−J_5, we express the energies of the ordered spin states in terms of the spin Hamiltonian

$$\hat{H} = -\sum_{i<j} J_{ij}\hat{S}_i\cdot\hat{S}_j \qquad (1)$$

where J_{ij} (= J_1, J_2, J_3, J_4, or J_5) refers to the SE parameter for the spin sites i and j. By application of the energy expressions obtained for spin dimers with N unpaired spins per spin site (in the present case, $N = 4$),[14] the total SE energies per eight FUs are written as

$$E(\text{FM}) = (-16J_1 - 8J_2 - 16J_3 - 16J_5 - 32J_4)(N^2/4)$$
$$E(\text{A0}) = (-16J_1 - 8J_2 - 16J_3 - 16J_5 + 32J_4)(N^2/4)$$
$$E(\text{A1}) = (+16J_1 - 8J_2 + 16J_3 - 16J_5)(N^2/4)$$
$$E(\text{A1}*) = (+16J_1 - 8J_2 + 16J_3 + 16J_5)(N^2/4)$$
$$E(\text{A2}) = (-16J_1 + 8J_2 + 16J_3 - 16J_5 - 32J_4)(N^2/4)$$
$$E(\text{A3}*) = (+16J_1 + 8J_2 - 16J_3 + 16J_5)(N^2/4) \qquad (2)$$

Thus, by equating the relative energies of the ordered spin states from the GGA + U calculations to the corresponding energy differences from the total SE energies, we obtain the values of J_1−J_5 listed in Table 2. The nearest-neighbor (NN) exchanges J_1 and J_2 are the two strongest AFM interactions. Compared with J_1 and J_2, the next NN exchange J_3 is negligible so that, practically, there is no spin frustration within each spin ladder. The interladder SE parameter J_5 along the a direction is substantial, which will lead to a strong AFM coupling between the spin ladders along the a direction. J_1, J_2, and J_5 of $Sr_3Fe_2O_5$ are comparable in magnitude to the corresponding SEs of $SrFeO_2$[13] and form 2D slabs of spin ladders parallel to the ab plane (hereafter, ∥ab slabs). The interladder exchange J_4 between adjacent ∥ab slabs along the c direction is extremely weak so that the spin−lattice of $Sr_3Fe_2O_5$ is practically 2D in nature. In agreement with the experiment,[8] the 3D AFM structure predicted from J_1, J_2, and J_5 is a ($2a$, $2b$, c) superstructure, regardless of whether J_4 is FM or AFM.

(14) (a) Dai, D.; Whangbo, M.-H. *J. Chem. Phys.* **2001**, *114*, 2887. (b) Dai, D.; Whangbo, M.-H. *J. Chem. Phys.* **2003**, *118*, 29.

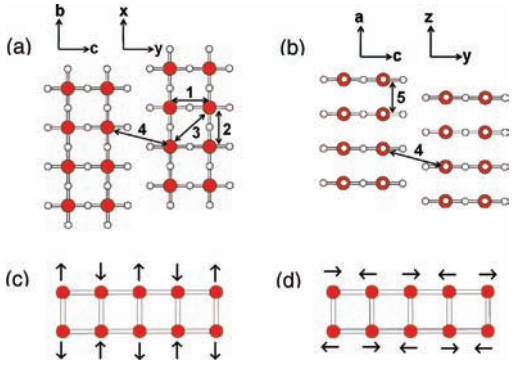

Figure 2. Fe_2O_5 spin ladders and spin orientations in $Sr_3Fe_2O_5$: (a) ab-plane projectional views of the Fe_2O_5 spin ladders; (b) ac-plane projectional views of the Fe_2O_5 spin ladders; (c) observed ∥c spin orientation in each Fe_2O_5 spin ladder; (d) hypothetical ∥b spin orientation in each Fe_2O_5 spin ladder. The numbers 1−5 in parts a and b represent the SE paths J_1, J_2, J_3, J_4, and J_5, respectively.

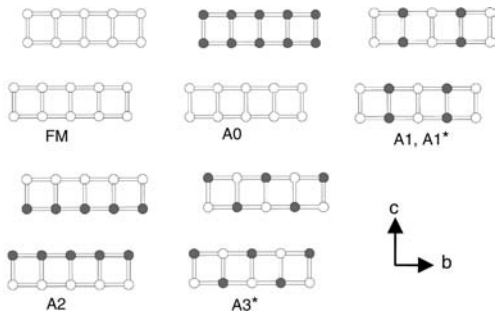

Figure 3. bc-plane projectional views of the six ordered spin arrangements of $Sr_3Fe_2O_5$ employed for the extraction of the five SE parameters J_1−J_5. Between adjacent sheets of spin ladders along the a direction, the spin arrangement has the FM coupling in the FM, A0, A1, and A2 and states but the AFM coupling in the A1* and A3* states.

Table 1. Relative Energies of the Six Ordered Spin States of $Sr_3Fe_2O_5$ (meV per Eight FUs) Determined from GGA + U Calculations

FM	1393.58	A1*	337.30
A0	1394.82	A2	935.81
A1	527.35	A3*	0.00

Table 2. Values of J_1−J_5 (in k_BK) Determined from GGA + U Calculations

J_1	−73.92	J_4	0.06
J_2	−70.42	J_5	−17.22
J_3	−4.64		

Between adjacent ∥ab slabs, the paths J_2 and J_4 form isosceles triangles (J_2, J_4, and J_4; Figure 2a) and the paths J_5 and J_4 also form isosceles triangles (J_5, J_4, and J_4; Figure 2b). Given that J_2 and J_5 are AFM, therefore, the interslab interactions are frustrated regardless of whether J_4 is FM or AFM. Consequently, the interslab interaction J_4 cannot bring about a 3D AFM ordering for $Sr_3Fe_2O_5$. We verify this conclusion by calculating the 3D AFM ordering temperature (T_N) of $Sr_3Fe_2O_5$ in terms of J_1−J_5 on the basis of the Monte Carlo (MC) simulation method used to calculate T_N of $SrFeO_2$.[13] As expected, our MC simulation shows that $Sr_3Fe_2O_5$ does not undergo a 3D ordering, regardless of the sign and strength of J_4. This means that $Sr_3Fe_2O_5$ cannot undergo a 3D AFM ordering in terms of SE interactions alone.

To examine why the spin orientation of $Sr_3Fe_2O_5$ prefers the c direction, we carry out GGA + U + SOC calculations

Table 3. Relative Energies (in meV per Eight FUs) of the ∥*a*, ∥*b*, and ∥*c* Spin Orientations of the Magnetic Ground State A3* Calculated from the GGA + *U* + SOC Calculations and from the MDD Interaction Energies

	SOC	MDD
∥*a*	1.843	0.258
∥*b*	0.217	0.102
∥*c*	0.000	0.000

for three spin orientations of the magnetic ground state A3*, namely, the spin orientations along the *a*, *b*, and *c* directions (hereafter referred to as the ∥*a*, ∥*b*, and ∥*c* spin orientations, respectively). For these GGA + *U* + SOC calculations, we reached the SCF energy convergence of 10^{-4} meV for the ∥*a*, ∥*b*, and ∥*c* spin orientations. Our calculations show that the ∥*b* and ∥*c* spin orientations are more stable than the ∥*a* spin orientation by 1.63 and 1.84 meV per eight FUs, respectively (Table 3). This is consistent with the experiment in that the spin orientation is predicted to be perpendicular to the *a* axis. To explain the latter, we consider the effect of SOC at each high-spin Fe^{2+} d^6 site by employing two independent coordinate systems for the orbital and spin angular momentum operators, e.g., (x, y, z) for $\hat{L}$ and (x', y', z') for $\hat{S}$. If the z' axis of the spin (i.e., the preferred spin orientation) is specified by the polar angles θ and ϕ of the (x, y, z) coordinate system, the SOC operator $\hat{H}_{SOC} = \lambda \hat{S} \cdot \hat{L}$ is given by[1,2]

$$\hat{H}_{SOC} = \lambda \hat{S}_{z'} \left(\hat{L}_z \cos\theta + \frac{1}{2}\hat{L}_+ e^{-i\phi} \sin\theta + \frac{1}{2}\hat{L}_- e^{i\phi} \sin\theta \right) + \frac{\lambda}{2}\hat{S}_{+'} \left(-\hat{L}_z \sin\theta - \hat{L}_+ e^{-i\phi} \sin^2\frac{\theta}{2} + \hat{L}_- e^{i\phi} \cos^2\frac{\theta}{2} \right) + \frac{\lambda}{2}\hat{S}_{-'} \left(-\hat{L}_z \sin\theta + \hat{L}_+ e^{-i\phi} \cos^2\frac{\theta}{2} - \hat{L}_- e^{i\phi} \sin^2\frac{\theta}{2} \right) \quad (3)$$

where the expressions of the first line are the spin-conserving terms, while those of the second and third lines are the spin-non-conserving terms. Given the SOC as the perturbation, the occupied d states ϕ_{occ} of each Fe^{2+} site can interact with the unoccupied d states ϕ_{unocc} to lower the energy by

$$\langle \phi_{occ} | \hat{H}_{SOC} | \phi_{unocc} \rangle^2 / \Delta E \quad (4)$$

where $\Delta E = E_{occ} - E_{unocc}$ and E_{occ} and E_{unocc} are the energies of ϕ_{occ} and ϕ_{unocc}, respectively. The most important states for this energy lowering are the ones with the smallest energy gap ΔE. Figure 4 shows the plots of the partial density of states (PDOS) obtained for the Fe d states in the magnetic ground state A3* from GGA + *U* calculations. As expected for the high-spin d^6 ion, all up-spin d states of Fe^{2+} are occupied. Among the down-spin d states, the z^2 state is occupied, as is also found for $SrFeO_2$.[13]

Thus, the smallest ΔE occurs within the down-spin d states so that only the spin-conserving part of the SOC is important, hence leading to the approximation[1,13]

$$\hat{H}_{SOC} \approx \lambda \hat{S}_{z'} \left(\hat{L}_z \cos\theta + \frac{1}{2}\hat{L}_+ e^{-i\phi} \sin\theta + \frac{1}{2}\hat{L}_- e^{i\phi} \sin\theta \right) \quad (5)$$

Consequently, only the $\langle z^2\downarrow | \hat{H}_{SOC} | xz\downarrow \rangle$ and $\langle z^2\downarrow | \hat{H}_{SOC} | yz\downarrow \rangle$ terms can be nonzero, and their values are maximum when $\theta = 90°$. This explains why the spin orientation is perpendicular to the *z* direction (i.e., perpendicular to the *a* axis).

Our GGA + *U* + SOC calculations predict that the ∥*c* spin orientation is slightly more stable than the ∥*b* spin orientation (Table 3). This is so because the $xz\downarrow$ band is slightly wider than the $yz\downarrow$ band due to the fact that the spin ladder chain runs along the *x* direction. To see how the observed ∥*c* spin orientation is enhanced by the MDD interactions, we calculate the MDD interaction energies for the ∥*a*, ∥*b*, and ∥*c* spin orientations of the magnetic ground state A3* of $Sr_3Fe_2O_5$. With $g = 2$, $S = 2$, and $(g\mu_B)^2/a_0^3 = 0.725$ meV, we calculate the MDD interaction energies, per eight FUs, for the ∥*a*, ∥*b*, and ∥*c* spin orientations by summing up all of the MDD terms whose distances r_{ij} are shorter than a cutoff distance r_c. Our calculations of the MDD interaction energies converge quickly as r_c is increased (see Figure S1 of the Supporting Information). When $r_c = 265$ Å, the MDD interaction energies are calculated to be accurate within 0.2×10^{-4} meV. In terms of the MDD interactions (Table 3), the ∥*c* spin orientation is favored over the ∥*b* spin orientation by 0.10 meV per eight FUs, which is, in turn, favored over the ∥*a* spin orientation by 0.16 meV per eight FUs (Table 3). The MDD interaction prefers the spin orientation perpendicular to the *a* axis, although its effect is much weaker than the SOC effect. As for the ∥*c* vs ∥*b* spin orientation, the MDD interaction shows a slightly weaker (by a factor of 2) preference for the ∥*c* spin orientation than does the SOC (Table 3). Because SOC is a single-site interaction, it cannot determine the magnetic ordering between the antiferromagnetically ordered ∥*ab* slabs. It is the MDD interaction, being a long-range multisite interaction, that provides their 3D magnetic ordering. Thus, the MDD interaction is essential for the 3D magnetic ordering of $Sr_3Fe_2O_5$. For compounds crystallizing in the Ruddlesden−Popper-type layered perovskites (e.g., La_2CuO_4 and $Sr_3Mn_2O_7$), in which the SEs between adjacent layers are frustrated, their 3D long-range magnetic ordering should also be governed by a combined effect of the SOC and MDD interactions.

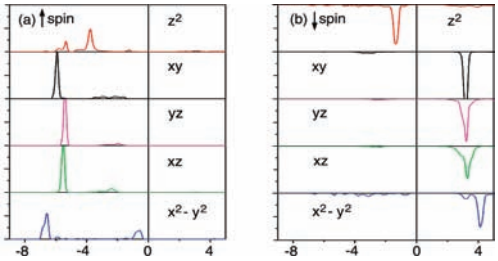

Figure 4. PDOS plots of the Fe 3d states obtained from GGA + *U* calculations for the magnetic ground state (i.e., the A3* state) of $Sr_3Fe_2O_5$. The coordinate for the orbitals is chosen such that the *x*, *y*, and *z* axes are parallel to the *b*, *c*, and *a* directions, respectively (see Figure 2). The energy scale is in electronvolts. The DOS scale covers 4.5 states/eV/atom for each up-spin PDOS plot and 3.0 states/eV/atom for each down-spin PDOS plot.

In summary, the spin−lattice of $Sr_3Fe_2O_5$ is 2D in nature in terms of its SE interactions but undergoes a 3D magnetic ordering as a consequence of the combined effect of the SOC and MDD interactions.

Acknowledgment. M.-H.W. thanks the U.S. Department of Energy for financial support (Grant DE-FG02-86ER45259) and computer resources at the NERSC Center and R. K. Kremer for invaluable discussion. H.-J.K. thanks the Korean Research Foundation (Grant KRF-2007-C00028; MOEHRD, Basic Research Promotion Fund).

Supporting Information Available: MDD interaction energies (Figure S1). This material is available free of charge via the Internet at http://pubs.acs.org.